

Development and Validation of an Ammonia (NH₃) Gas Concentration Measurement Device for Industrial and Health Application

Y. Abdullahi¹, I. G. Saidu², M. B. Abdullahi³, and K. A. Dabai⁴

¹Department of Applied Physics, Umaru Ali Shinkafi Polytechnic Sokoto, Nigeria

^{2,3}Department of Physics, Usmanu Danfodiyo University, Sokoto, Nigeria

⁴Department of Electrical Engineering, Usmanu Danfodiyo University, Sokoto, Nigeria

DOI: <https://doi.org/10.51584/IJRIAS.2025.100700017>

Received: 25 June 2025; Accepted: 02 July 2025; Published: 31 July 2025

ABSTRACT

Ammonia (NH₃) is a harmful air pollutant that not only contributes to environmental damage but also poses serious health risks, particularly in confined or poorly ventilated spaces like farms, waste management facilities, and industrial settings. Monitoring ammonia levels accurately is essential for protecting both the environment and public health. This study focuses on creating a cost-effective, real-time monitoring system designed to detect ammonia in the air. The system integrates the MQ135 gas sensor and the DHT11 temperature and humidity sensor with an Arduino Mega 2560 microcontroller. By tracking ammonia levels along with temperature and humidity, the device offers a more complete view of air quality conditions. Before physical testing, the system was validated through circuit simulation to ensure proper communication between components, identify any circuit issues, and assess the performance of the signal processing algorithm. Calibration was a key part of development, aimed at improving accuracy across various ammonia concentration levels while considering environmental fluctuations. Lab tests showed that the MQ135 sensor produced consistent results with low noise, achieving an average error margin of just 2.11%. The most accurate readings were observed within the 20–45 ppm range. Incorporating temperature and humidity data from the DHT11 sensor opens the door to future enhancements, such as environmental compensation algorithms. Overall, the system proved effective for general air quality monitoring, with potential for future upgrades like automatic calibration and support for detecting multiple gases

Keywords: MQ135 sensor, Ammonia, Gas sensor, Arduino mega 2560, Microcontroller

BACKGROUND TO THE STUDY

Ammonia (NH₃) is a common air pollutant released from both natural processes and human activities. It plays an important role in the nitrogen cycle and atmospheric chemistry, contributing to the formation of secondary particulate matter—like ammonium salts—which can reduce air quality, impair visibility, and harm human health (Behera *et al.*, 2013). Agriculture is one of the main contributors to ammonia emissions, with key sources including livestock waste, fertilizer use, and the decomposition of organic material (Ti *et al.*, 2019). In fact, the European Environment Agency reports that agriculture accounts for more than 90% of ammonia emissions in most developed countries (EEA, 2020; Murawska and Prus, 2021). In enclosed settings like poultry farms, greenhouses, and waste treatment plants, ammonia levels can quickly exceed safe limits, potentially causing respiratory issues, reducing productivity, and leading to long-term health problems for both humans and animals (Wyer *et al.*, 2022).

With growing awareness of these impacts, there is an increasing demand for practical and affordable methods to monitor ammonia levels. Traditional detection techniques such as spectrophotometry, gas chromatography,

and ion-selective electrodes offer high precision but are often expensive, complex, and slow due to lengthy sample preparation and processing times (Koel and Kaljurand, 2019). In response, low-cost gas sensors like the MQ135 have emerged as promising alternatives for real-time ammonia detection. The MQ135 is a metal oxide semiconductor (MOS) sensor capable of detecting a range of gases, including ammonia, by monitoring changes in its electrical resistance when exposed to target compounds. While it's a general-purpose sensor, it can be calibrated to reliably measure ammonia, making it suitable for environmental applications (Seesaard *et al.*, 2024).

Microcontrollers like the Arduino Mega 2560 are widely used in these types of embedded systems. Acting as the system's control unit, the Arduino processes sensor data, manages signal interpretation, and outputs readings. Thanks to its ample memory, numerous input/output pins, and user-friendly programming environment, the Arduino Mega is well-suited for integrating multiple sensors and building custom monitoring tools (Barrett, 2020). Its open-source design makes it especially appealing for researchers, educators, and field professionals who need flexible, cost-effective solutions (Pecly, 2023). When paired with gas sensors, it enables the creation of portable, scalable devices that can deliver near real-time air quality data without the need for lab-grade infrastructure (Akinwumi *et al.*, 2024).

A crucial part of working with sensors like the MQ135 is calibration. Because the relationship between gas concentration and sensor resistance is non-linear, a logarithmic approach is often used to create an accurate response curve. This involves measuring the ratio of sensor resistance (R_s) to its baseline value (R_0) across known ammonia concentrations. Doing so enhances the sensor's reliability in diverse environments (Carrillo *et al.*, 2020).

Several research efforts have explored low-cost gas detection systems using MQ-series sensors with various Arduino boards. For example, Mane *et al.*, (2020) and Abbas *et al.*, (2021) developed air quality monitors using the MQ135 with Arduino Uno. However, the Arduino Mega offers better hardware support, with more memory, I/O pins, and communication ports. Petric *et al.*, (2019) found large measurement errors up to 33% when using the MQ137 sensor without adequate calibration, underscoring the importance of this step. Other researchers like Mohiddin and Kumar (2018), and Carrill *et al.*, (2020), calibrated sensors using factory-provided data, though these values often fall short under real-world conditions. Maulini *et al.*, (2022) tracked ammonia in aquaponic systems but did not address long-term sensor drift or interference from other gases. Mondal and Banerjee, (2022) presented an IoT-based system using NodeMCU, but its complexity may make it less accessible to users without technical expertise. Many of these studies also relied on the Arduino Uno, which can limit scalability and data processing capabilities.

Although these projects provide valuable insights, many lack robust calibration tailored to specific environments, and few include simulation-based validation before real-world deployment. These gaps highlight the need for more reliable, scalable, and well-calibrated monitoring systems an issue this study aims to address.

Building on previous work, this research presents a real-time ammonia monitoring system using the MQ135 gas sensor integrated with an Arduino Mega 2560. The goal is to deliver a low-cost, accurate, and scalable solution suitable for both environmental monitoring and industrial applications.

System Design

Block Diagram of the System

The aim of the study is to develop an embedded system capable of measuring the concentration of ammonia gas in air. For this purpose, we require a gas sensor to detect the amount of gas in air. Secondly the amount of ammonia gas measured needs to be display necessitating a display unit. Because the performance of gas sensors is highly affected by temperature and humidity a thermometer and a hygrometer are also necessary. To control the activities of all the sections, a microcontroller was employed, Finally, an appropriate power supply is needed to power all the sections. The general requirement is summed up in the block diagram representation of Figure 1.

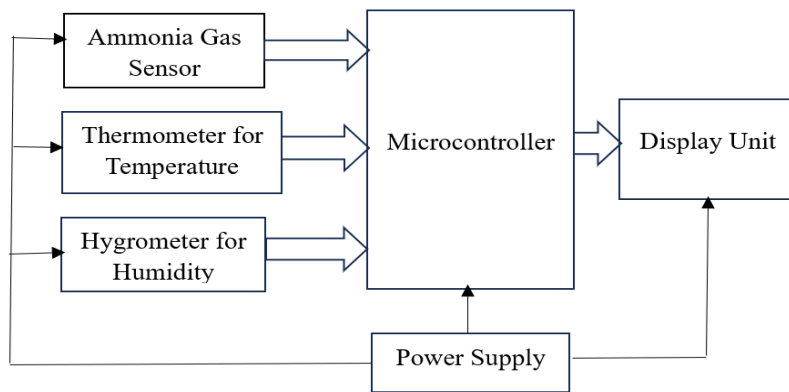


Figure 1: Block Diagram of the NH₃ Air Quality Monitoring System

Circuit Design

Gas sensor circuit design

A gas sensor, also known as a gas detector, is a device used to identify and measure the concentration of gases in the surrounding air. These sensors play a key role in a variety of settings, including safety systems, environmental monitoring, industrial operations, and indoor air quality control (Eranna, 2011). They are capable of detecting a range of harmful gases such as carbon monoxide (CO), nitrogen dioxide (NO₂), and sulfur dioxide (SO₂). Gas sensors come in different types, each designed based on specific sensing principles and suited for different applications. Some common types include Electrochemical Sensors, Infrared (IR) Sensors, Photoionization Detectors (PID), Catalytic Bead Sensors, Colorimetric Tubes, and Metal Oxide Semiconductor (MOS) Sensors (Li, 2015).

Among these, MOS sensors are particularly popular due to their many advantages. They offer high sensitivity, can detect a broad range of gases, and respond quickly to changes in gas concentration (Eranna, 2011). Their simple design allows for easy miniaturization and mass production, making them affordable and widely available. Additionally, they typically consume low power, integrate well with electronic systems, and deliver stable and repeatable readings over time (Eranna, 2011; Altawell, 2021). Because of these strengths, a MOS sensor was selected for use in this project.

One of the most widely used MOS-based gas sensors is the MQ135. It stands out for its ability to detect multiple gases, high sensitivity, fast response and recovery times, and a long operational life all at a relatively low cost. It also provides both analog and digital outputs, includes a built-in heater element, and operates within a broad detection range (typically 10–1000 ppm depending on the specific gas). The sensor requires a short preheating period and operates at standard voltages, making it ideal for embedded systems and environmental monitoring applications (Wijaya, Sarno *et al.*, 2016; Chodorek *et al.*, 2022). The pin configuration for the MQ135 is shown in Figure 2.

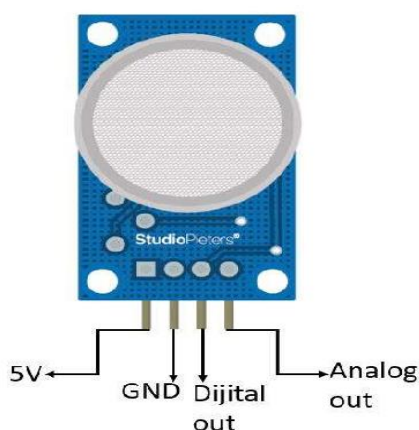


Figure 2: Pin Configuration of MQ135 Sensor (Azemi, Loon *et al.*, 2021)

The controller chosen for this project is the Arduino Mega 2560. Compared to the Arduino Uno and other smaller Arduino boards, the Mega offers several advantages that make it more suitable for larger and more complex applications. It comes with significantly more memory, a greater number of input/output pins, and multiple serial communication ports (UARTs). These features allow for better scalability and more flexibility in handling advanced tasks, making it a strong choice for this design (Rico and Turkoglu, 2016). To monitor air quality, the MQ135 gas sensor was connected to the Arduino Mega. The sensor's VCC pin was wired to the 5V output of the Arduino, while its GND pin was connected to one of the Arduino's ground (GND) terminals. The analog output of the sensor (A0) was linked to the A0 analog input on the Arduino Mega, allowing it to read air quality data. The digital output of the MQ135 was not used in this setup. According to the sensor's datasheet, a load resistor (RL) between 10K and 47K ohms is recommended for proper operation (MQ135 datasheet, 2023). In this design, a 47K ohm resistor was selected and connected between the sensor's analog output and ground. This setup is illustrated in Figure 3.

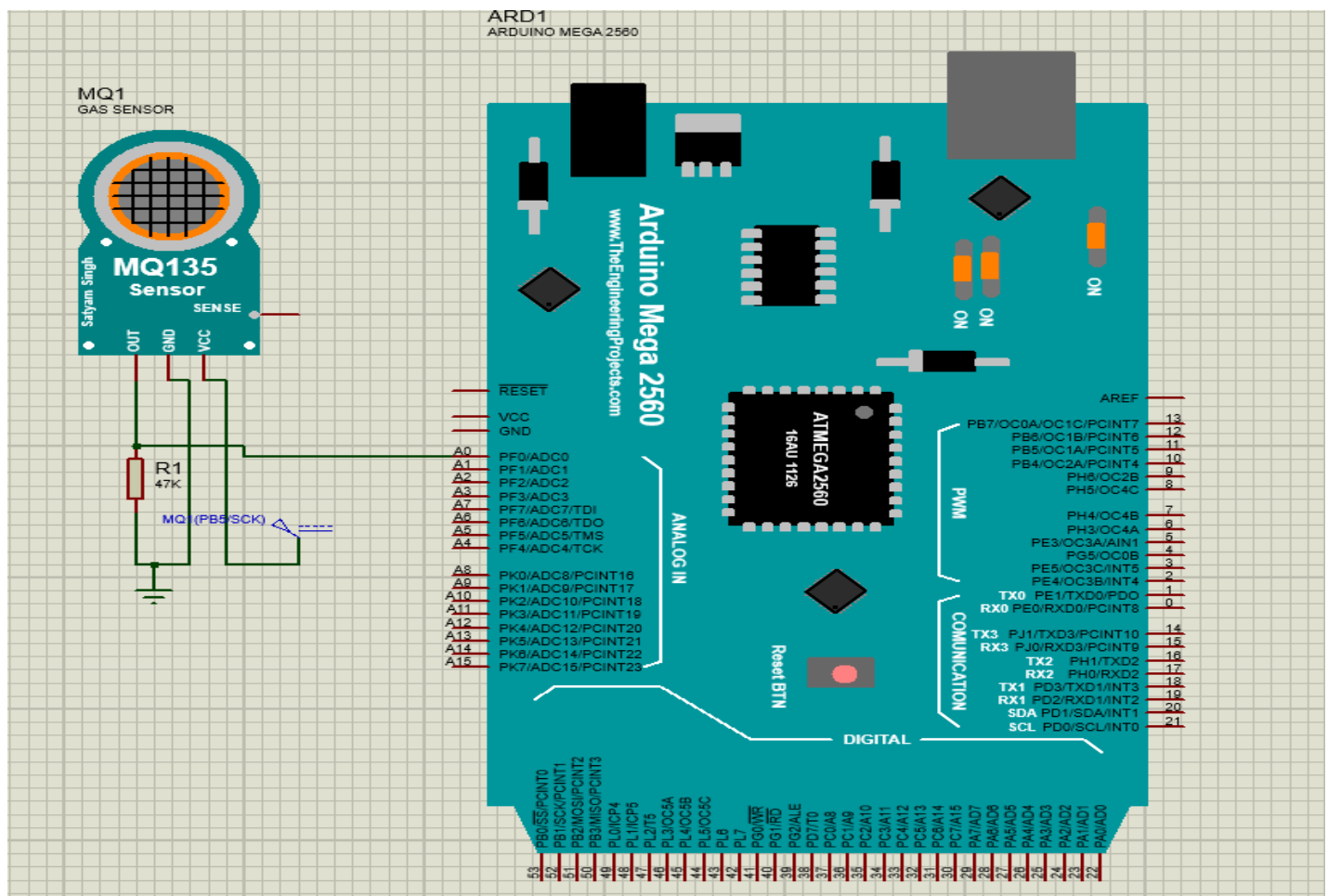


Figure 3: MQ135 Gas Sensor Circuit Design

Display Unit Design

A 16x2 LCD display was used in this project to show the measured ammonia gas concentration in real time. This display, equipped with an I2C interface, was connected to the Arduino Mega using the following configuration: the Register Select (RS) pin was connected to digital pin 12 on the Arduino, and the Enable (E) pin was connected to pin 11. The data pins D4 through D7 were connected to digital pins 5, 4, 3, and 2, respectively. The LCD's VCC pin was connected to the Arduino's 5V output, while GND was connected to the ground (GND) pin.

In addition, the LCD's K, RW, and VSS pins were also grounded. To control the contrast of the display, a potentiometer was included in the circuit. The potentiometer's negative terminal was connected to ground, while the VDD and positive terminal were connected to the 5V supply from the Arduino. The complete wiring setup is illustrated in Figure 4.

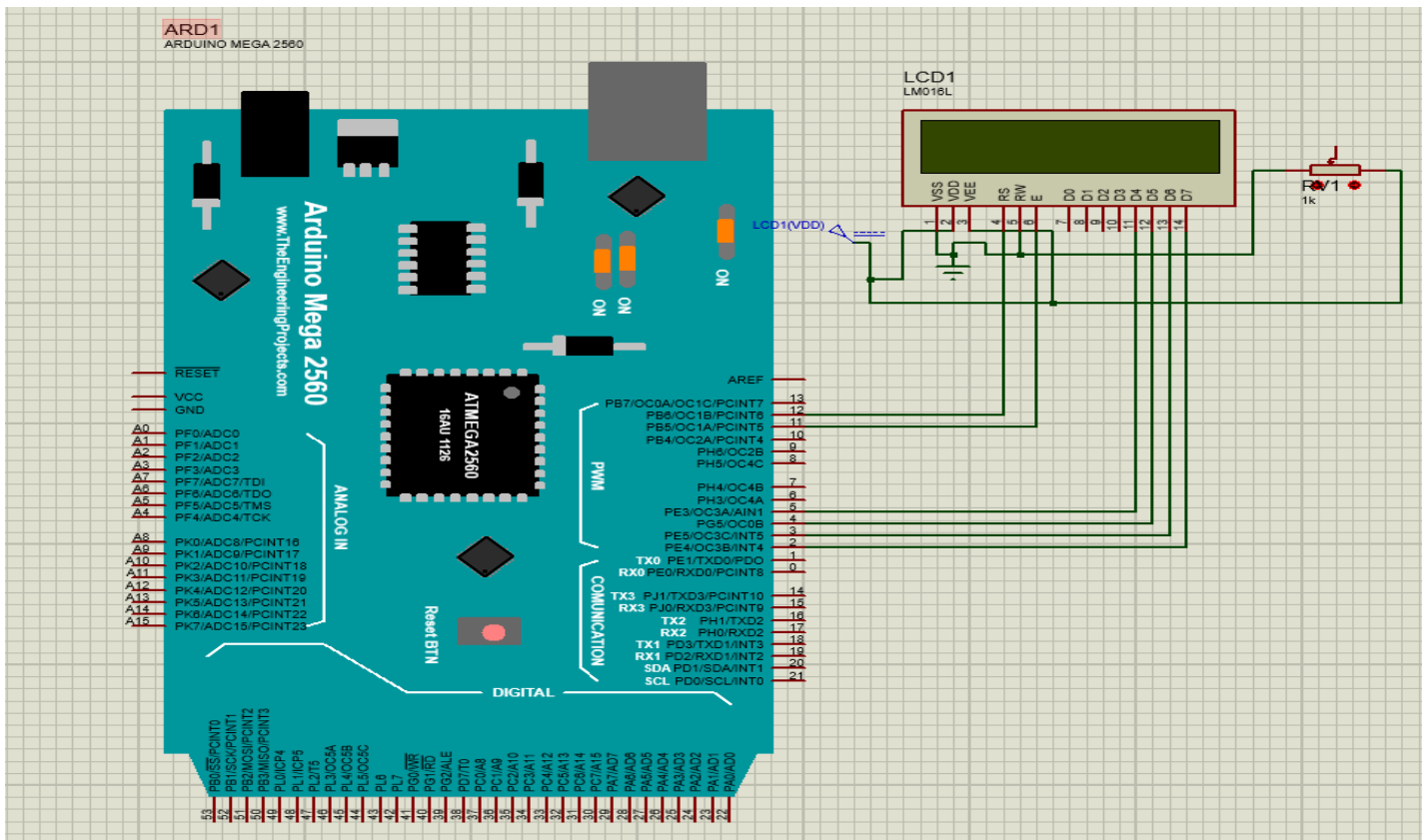


Figure 4: 16x2 LCD Circuit Design

Thermometer and Hygrometer Circuit Design

Since temperature and humidity can significantly affect the performance of the MQ135 gas sensor, it was important to include sensors that could monitor these environmental conditions to ensure accurate readings. While separate temperature (thermometer) and humidity (hygrometer) sensors are available, using them individually would require more space and make the integration process more complex. To simplify the design, the DHT11 sensor was selected. The DHT11 is a compact module that combines both temperature and humidity sensing in a single unit. It offers several advantages over traditional standalone instruments, including low cost, ease of use, low power consumption, and sufficient accuracy for applications like environmental monitoring, data logging, and automated alerts (Syahputra, Sihombing *et al.*, 2023; Siswanto *et al.*, 2019). These features made the DHT11 a practical and efficient choice for this project. The pin configuration of the DHT11 is illustrated in Figure 5.

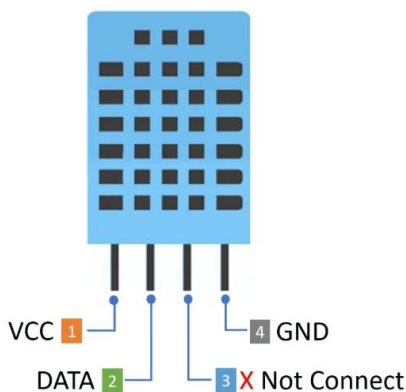


Figure 5: Pin Configuration of the DHT11 (Kuria *et al.*, 2020)

The DHT11 sensor was integrated to the controller by connecting its V_{CC} terminal to the 5V output of the Arduino Mega. Its GND is connected to the GND pin of the Arduino Mega. The data pin is connected to digital pin 7 on the Arduino Mega as shown in figure 6.

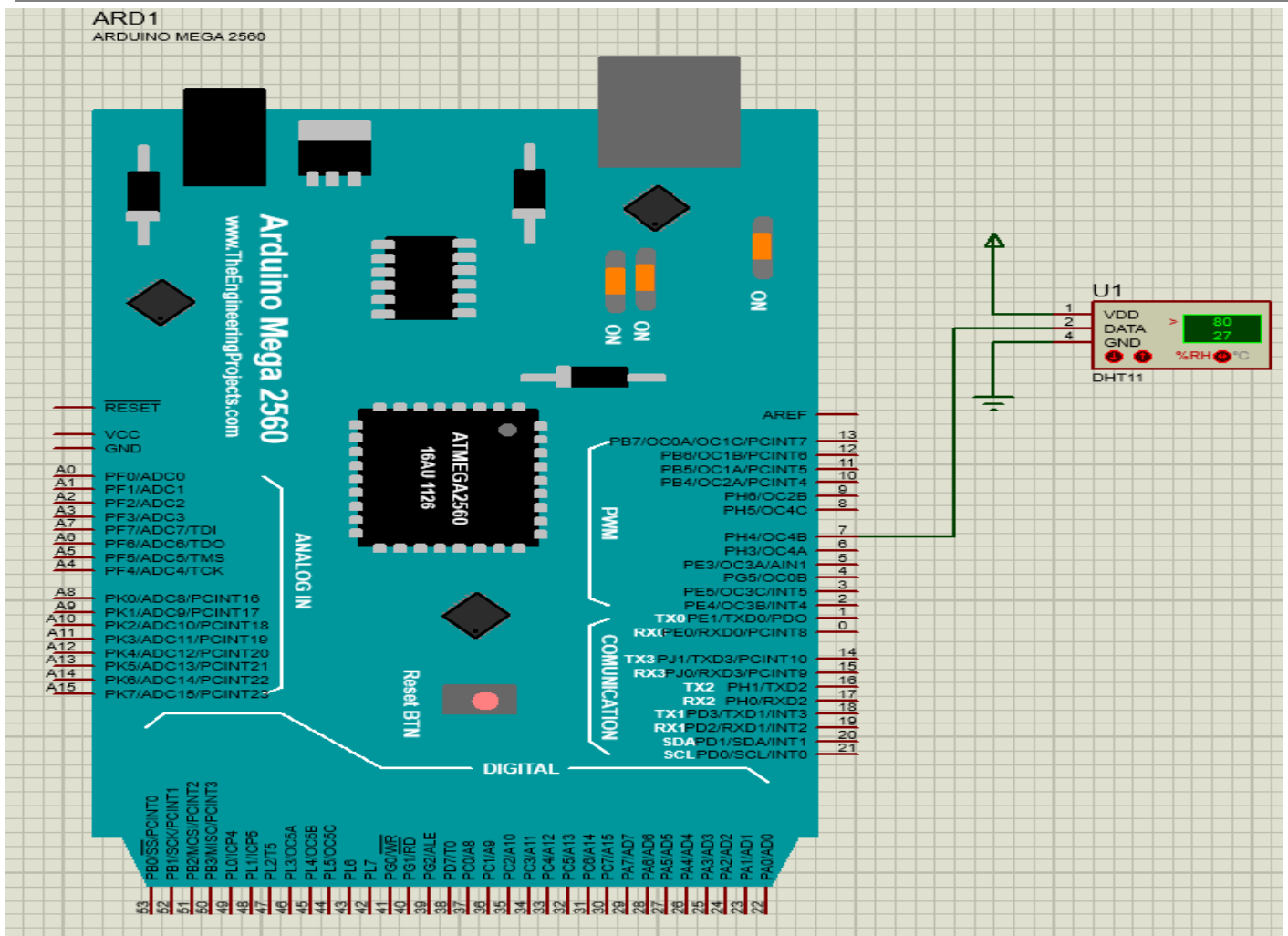


Figure 6: DHT11 Circuit Design

Power Supply Design

Every electronics system requires a well-regulated power supply. For our design all the sections require 5V dc. A 12V DC battery was obtained and regulated to 5 V using voltage regulator. The complete and schematic circuit design is shown in figure 7 and 8 respectively.

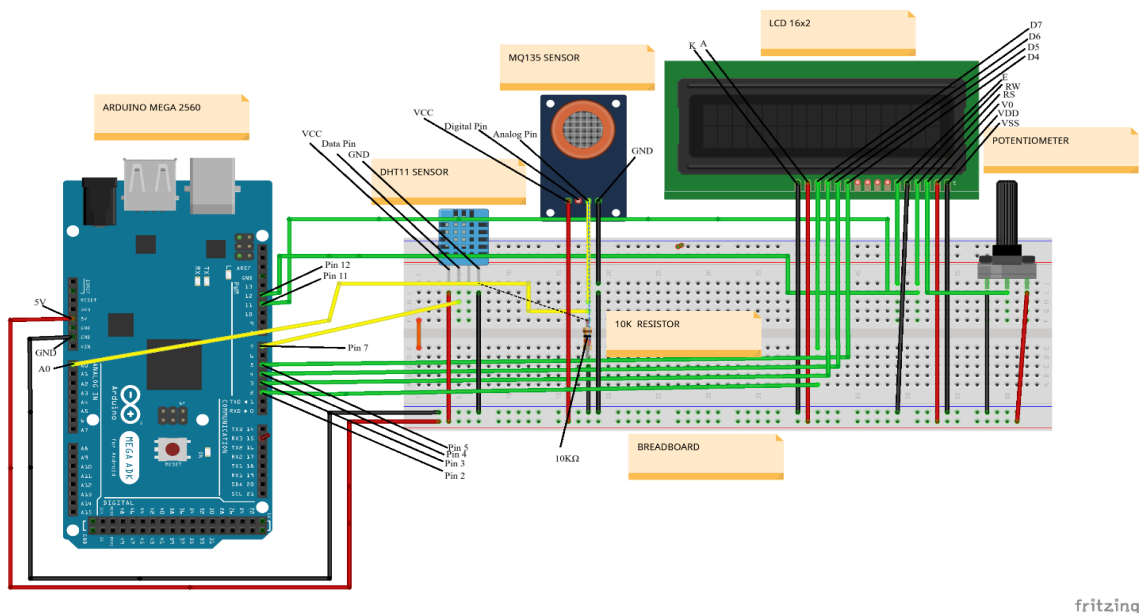


Figure 7: Complete Circuit Diagram of NH₃ Air Quality Monitoring System

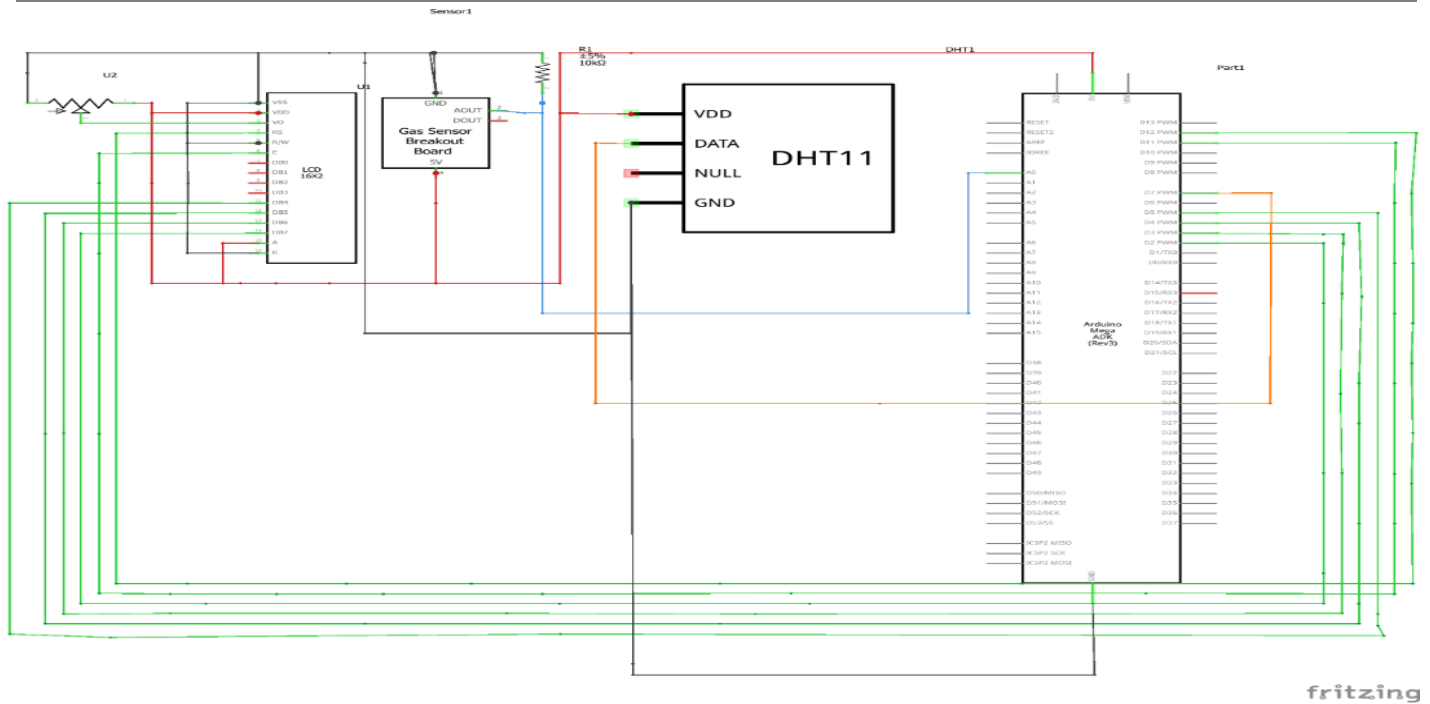


Figure 8: Schematic Circuit Diagram of NH₃ Air Quality Monitoring System

Setup Algorithm for Implemented Software

Figure 9 presents the complete flowchart explaining the operational logic of the Arduino code used in the NH₃ air quality monitoring system. The software integrates the MQ-135 gas sensor, DHT11 temperature and humidity sensor, and a 16x2 LCD display to continuously monitor and display ammonia (NH₃) concentration, ambient temperature, and humidity levels. The flowchart illustrates the step-by-step algorithm, including sensor initialization, data acquisition, analog-to-digital conversion, sensor calibration, data processing, and real-time display on the LCD. It also highlights how the Arduino Mega reads inputs from both sensors, computes the gas concentration using a mathematical formula based on R_s/R_o ratio, and transmits the processed data via serial communication for further analysis or logging.

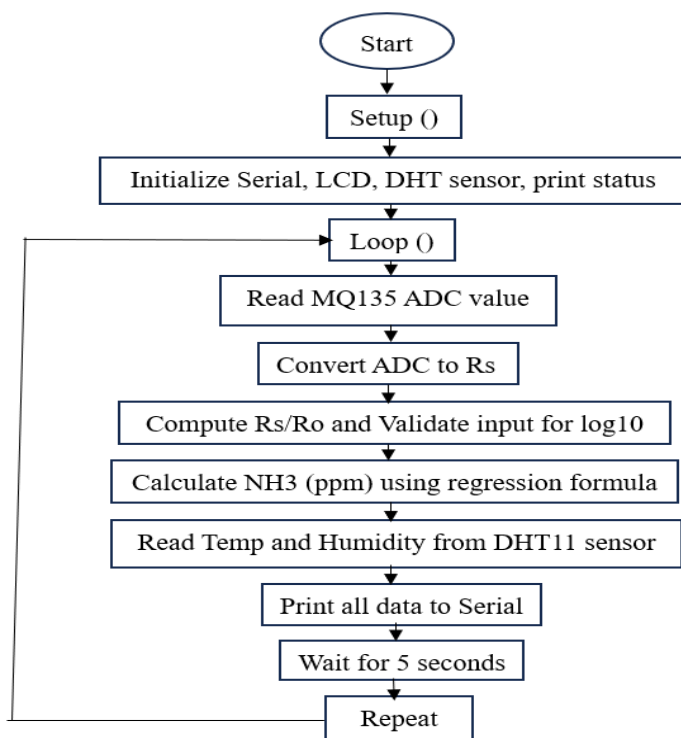


Figure 9: Flowchart of the Implemented Algorithm

Simulation of the Designed Circuit and Algorithm of the Implemented Software

To ensure proper component interaction, verify functionality, detect errors in the designed circuit, and test the accuracy, speed, and stability of the implemented algorithm, a simulation was carried out prior to physical implementation. This simulation was performed using Proteus software. After installing the necessary libraries, the Arduino code was written and compiled using the Arduino IDE. During compilation, a HEX file was automatically generated in the IDE's temporary directory, as shown in Figure 5. This HEX file was then copied from the temporary folder and pasted into the Program File field in the Arduino Mega 2560 Edit Component Dialog Box within Proteus, as illustrated in Figure 6. Upon pressing the play button in Proteus, the simulation began. The system successfully displayed real-time updates of analog readings (ADC values), ammonia gas concentration in parts per million (ppm), temperature, and humidity on both the LCD screen and the virtual terminal, with data refreshing every second as defined in the code, as shown in Figure 7. These observations confirm the successful interaction of the components, validate the functionality of the designed circuit, and demonstrate the accuracy, reliability, and stability of the implemented software algorithm.

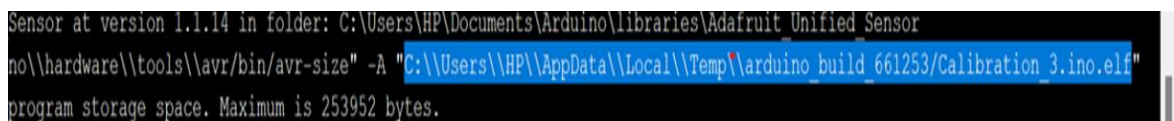


Figure 10: Hex File Generated in the Arduino IDE's Temporary Directory

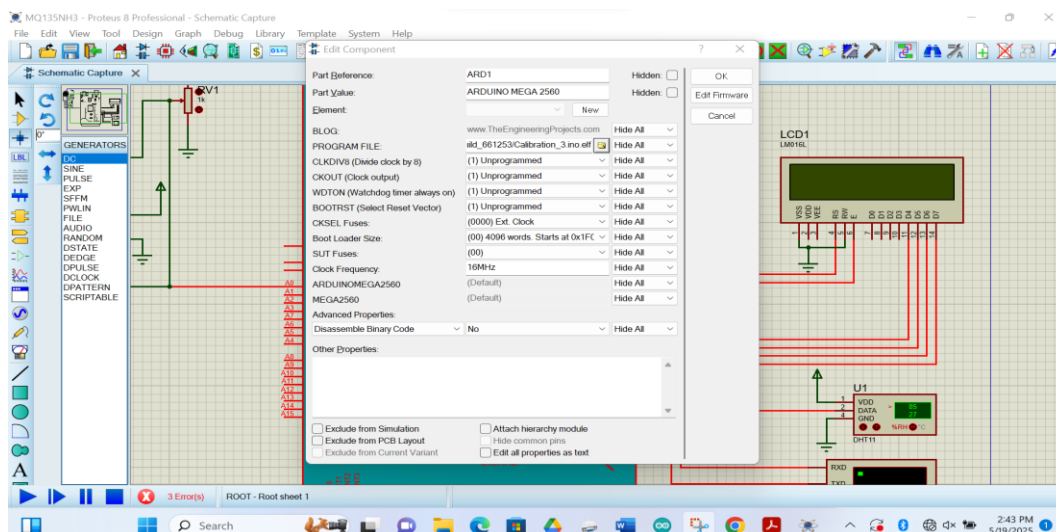


Figure 11: Generated Hex File Pasted into Program File Field in the Edit Component Dialog Box

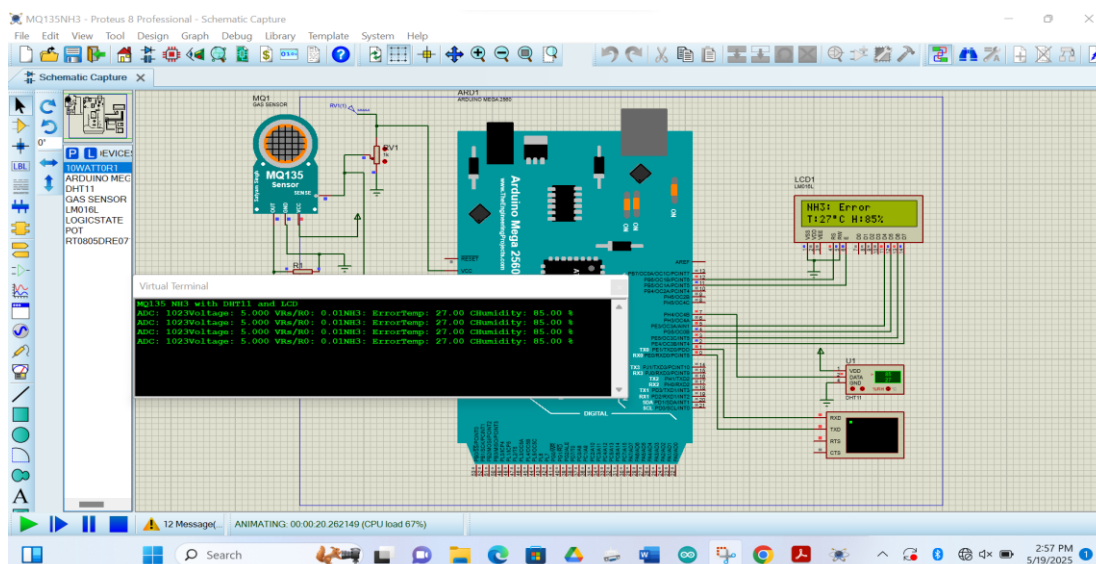


Figure 12: Circuit Designed and Algorithm Simulated Result

Calibration of the MQ-135 Gas Sensor For NH₃

The MQ-135 gas sensor requires calibration to ensure accurate measurements of ammonia (NH₃) concentration. The circuit diagram of the MQ135 sensor is shown in Figure 113. In operation a supply voltage of 5 V is connected as shown to both heat the heater and to power the sensor.

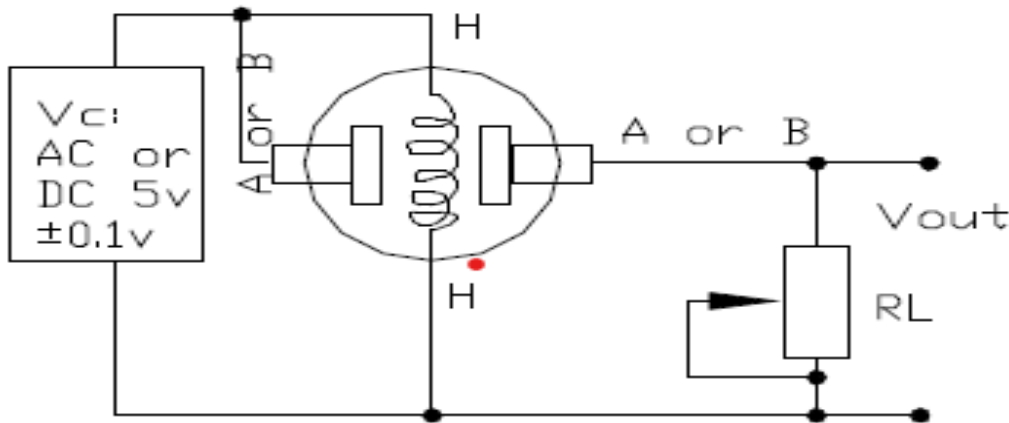


Figure 13: Electric Parameter Measurement Circuit (MQ135 datasheet,2022)

The sensors resistance normally changes with changes in concentration level of gas. The ratio of R_s to that of R_0 corresponds to the gas concentration level where R_0 is the sensor resistance in clean air and R_s is the resistance of gas sensor at any other concentration (targeted gas environment). To determine R_0 , the sensor resistance is measured in clean air to set the reference baseline resistance. Once R_0 is known, it can be used as a baseline reference in the sensor's equation to determine ammonia concentrations in different environments. Figure 14 shows the relationship between the ratio R_s/R_0 and the corresponding gas concentration in ppm. It shows the relationship for different gas concentrations.

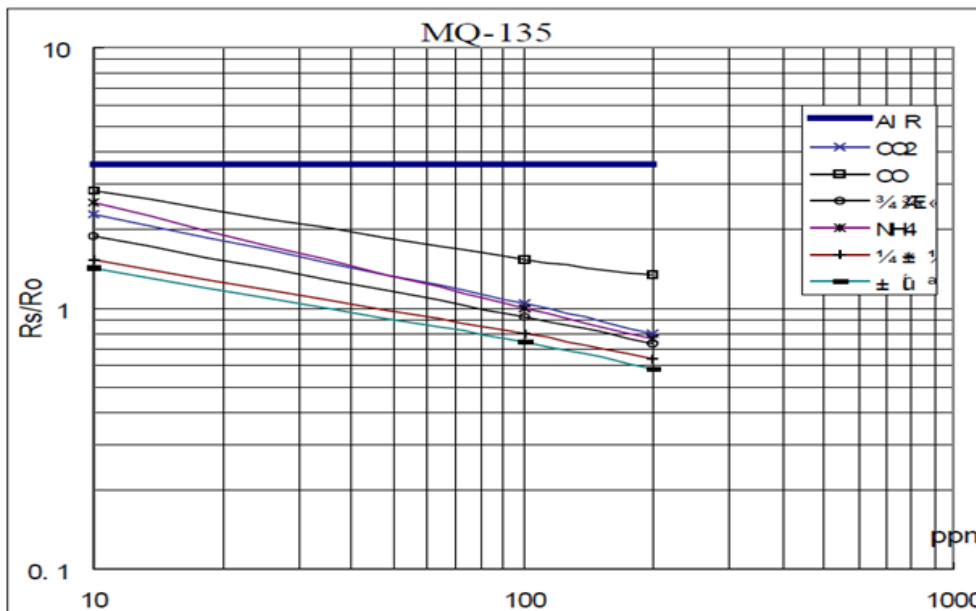


Figure 14: MQ135 Graph from Sensor's Datasheet (MQ-135 datasheet, 2022)

It could be deduced from the plots that $R_0 = \frac{R_s}{3.6}$ 1

So that the ratio of R_s to R_0 is approximately 3.6 in clean air. To calculate the sensor's resistance (R_s) values, we referred to the MQ135 datasheet, as shown in figure 13. The MQ135 sensor operates as part of a voltage divider circuit. The general formula for the output voltage across a resistor in a voltage divider circuit is given by (Salam and Rahman, 2018):

$$V_{out} = V_{in} \times \frac{R_{load}}{R_{total}}$$

2

Where:

- V_{in} is the input voltage (in this case, the supply voltage V_C),
- R_{load} is the resistor across which the output voltage is measured (in this case, R_L),
- R_{total} is the total resistance of the series resistive network, which is the sum of R_s (the sensor resistance) and R_L (the load resistance).

Applying the voltage divider formula in case of MQ135 sensor the output voltage across load resistor is:

$$V_{RL} = V_C \times \frac{R_L}{R_S + R_L}$$

3

This formula gives the relationship between the output voltage and the resistances in the voltage divider network. The sensor's resistance, R_s , is the key factor that varies with gas concentration, while R_L is typically fixed. The internal sensor resistance (R_s), can be solved from the equation (3) given as:

$$R_S = \frac{V_C \times R_L}{V_{RL}} - R_L$$

$$R_S = \left(\frac{V_C}{V_{RL}} - 1 \right) \times R_L$$

4

From the ongoing, it is seen that to evaluate R_s we measure V_{RL} and substitute in equation 4 since all other parameters are known. Therefore, an Arduino code was written to evaluate R_0 , and R_s based on the measured V_{RL} . Figure 15 shows a complete flowchart of the Arduino code.

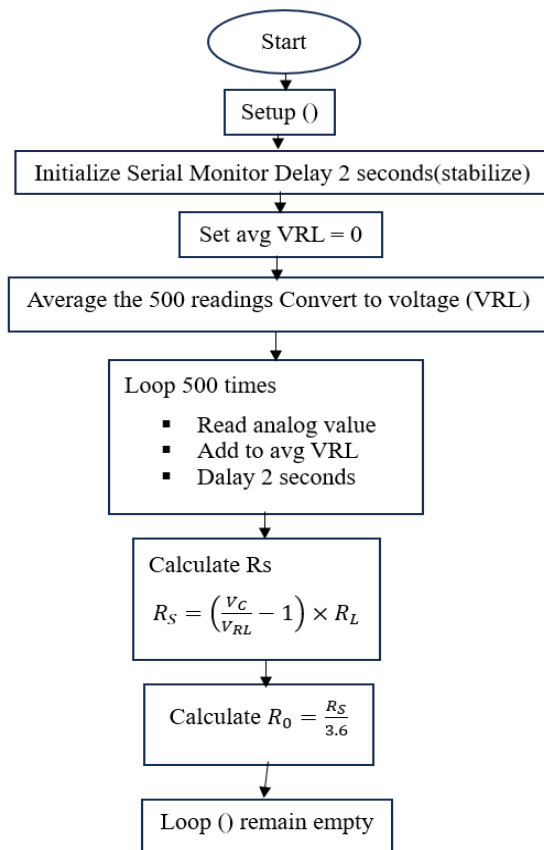


Figure 15: Flowchart for Calculation the Values of R_0 , R_s , And V_{RL}

A program was written in C++, and uploaded onto the controller. The circuit was assembled as shown in Figure 16. A fan was included to help distribute the gas evenly as suggested by (Ahmareza *et al.*, 2024).

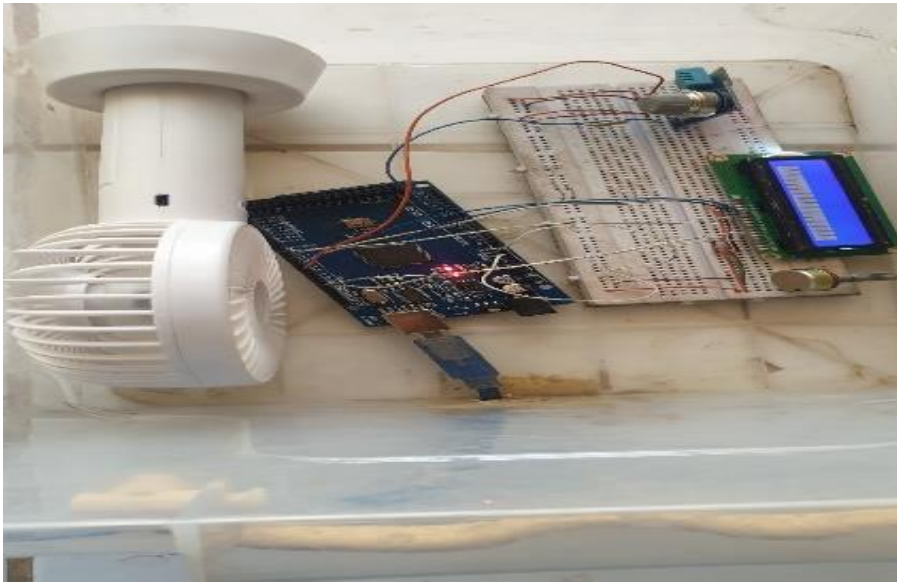


Figure 16: Connected circuit under test

Determination of base line resistance (R_0)

After assembling the circuit, the sensor was preheated for 24 hours as recommended in the MQ135 datasheet (MQ-135 datasheet, 2022). The voltage measured by the sensor was used to evaluate the resistance R_s denoted as R_0 as shown in Figure 15.

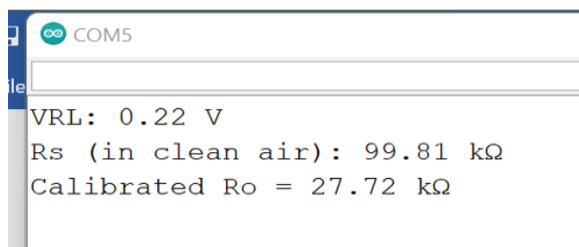


Figure 15: Resulting Values of R_0 , R_s , and V_{RL} on Arduino IDE's Serial Monitor

Determination of $\frac{R_s}{R_0}$ Values for other Known Concentration of NH_3

To prepare a desired standard solution, the process is to dilute a stock solution (pure solution) in water to achieve the target concentration. The dilution formula used is (Amin *et al.*, 2021):

$$C_1V_1 = C_2V_2 \quad 5$$

Where:

C_1 = Concentration of the stock solution ((in mg/ml or mg/l),

V_1 = Volume of the stock solution required (in mL)

C_2 = Desired concentration of the standard solution (in mg/L)

V_2 = Final volume of the diluted solution (in mL).

In this case we used the ammonia aqueous solution with specific gravity (SG) of 0.88, this means that, the ammonia solution is 0.88 times the density of water, since the density of water is approximately 1 g/mL , the

density of ammonia solution would be 0.88 g/mL (or 880 mg/mL) which is the ammonia stock solution. To achieve different concentrations of ammonia using the given formula, we ensured that we used a fixed volume of diluted solution (50 mL). The concentration of the stock ammonia is 880mg/mL. To obtain 1 ppm concentration of the ammonia we substitute the values into the dilution formula (Equation 5) to give:

$$(880 \text{ mg/mL}) \times V_1 = (1 \text{ mg/mL}) \times (50 \text{ mL})$$

$$V_1 = \frac{(1 \text{ mg/mL}) \times (50 \text{ mL})}{(880 \text{ mg/mL})}$$

$$V_1 = 0.057 \text{ mL} = 57 \mu\text{L}$$

Therefore, we measured 57 μL of the 880-ppm ammonia stock solution using a micropipette and add it to 49.43 mL of distilled water to make the total volume up to 50 mL, which corresponds to a concentration of 1 ppm. The same method was repeated to obtain other target concentrations (10 ppm, 20 ppm, 30 ppm, 40 ppm, and 50 ppm). The result of the different values of pure ammonia solution and the quantity of water is summed up in Table1.

Table 1: Target concentrations in ppm

Quantity of Ammonia (mL)	Quantity of Water (mL)	Concentration (ppm)
0.57	49.43	10
1.14	48.86	20
1.70	48.30	30
2.56	47.44	40
2.84	47.16	50

After obtaining the calibrated fresh air resistance values (R_o) as displayed in the Arduino IDE's Serial Monitor figure 15 the values were copied and pasted into the Arduino code for R_s/R_o Reading. The flowchart for the Arduino code related to this reading is shown in Figure16.

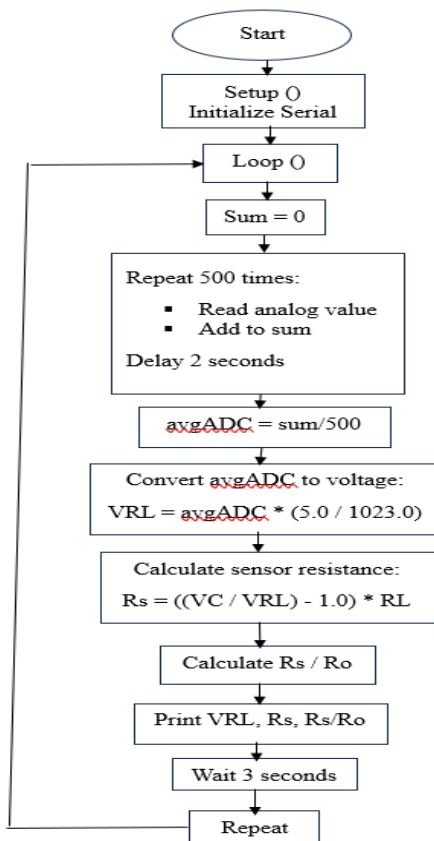


Figure 16: Flowchart for R_s/R_o Reading

After connecting the circuit, the code was uploaded to the Arduino board to measure the ratio of R_s to R_o . The system was allowed to warm up for a few minutes in a well-ventilated area. Then, a known NH_3 concentration of 10 ppm was exposed to the sensor's chamber, as shown in Fig. 15, and the sensor's chamber was enclosed, as shown in Fig. 16. It enclosed so that the concentration of the gas does not reduce if in the open air. The fan ensured that the gas is well distributed within the enclosure.



Figure 17: 10ppm Exposed to Sensor's Chamber



Figure 18: 10ppm Enclosed in Sensor's Chamber

The system was allowed to stabilize and the results of VRL, R_0 , R_s/R_0 was displayed on Arduino IDE's serial monitor as shown in figure 19.

COM5			
VRL:	0.41 V,	R_s :	53.23 k Ω , R_s/R_0 : 25.84
VRL:	0.41 V,	R_s :	53.18 k Ω , R_s/R_0 : 25.82
VRL:	0.41 V,	R_s :	53.21 k Ω , R_s/R_0 : 25.83
VRL:	0.41 V,	R_s :	53.23 k Ω , R_s/R_0 : 25.84
VRL:	0.41 V,	R_s :	53.19 k Ω , R_s/R_0 : 25.82
VRL:	0.41 V,	R_s :	53.30 k Ω , R_s/R_0 : 25.87
VRL:	0.41 V,	R_s :	53.27 k Ω , R_s/R_0 : 25.86
VRL:	0.41 V,	R_s :	53.26 k Ω , R_s/R_0 : 25.85
VRL:	0.41 V,	R_s :	53.20 k Ω , R_s/R_0 : 25.83
VRL:	0.41 V,	R_s :	53.26 k Ω , R_s/R_0 : 25.85
VRL:	0.41 V,	R_s :	53.30 k Ω , R_s/R_0 : 25.87
VRL:	0.41 V,	R_s :	53.31 k Ω , R_s/R_0 : 25.88
VRL:	0.41 V,	R_s :	53.32 k Ω , R_s/R_0 : 25.88
VRL:	0.41 V,	R_s :	53.29 k Ω , R_s/R_0 : 25.87
VRL:	0.40 V,	R_s :	53.34 k Ω , R_s/R_0 : 25.89
VRL:	0.41 V,	R_s :	53.26 k Ω , R_s/R_0 : 25.85
VRL:	0.41 V,	R_s :	53.24 k Ω , R_s/R_0 : 25.85
VRL:	0.41 V,	R_s :	53.30 k Ω , R_s/R_0 : 25.87
VRL:	0.41 V,	R_s :	53.28 k Ω , R_s/R_0 : 25.86
VRL:	0.41 V,	R_s :	53.26 k Ω , R_s/R_0 : 25.85
VRL:	0.40 V,	R_s :	53.36 k Ω , R_s/R_0 : 25.90
VRL:	0.41 V,	R_s :	53.30 k Ω , R_s/R_0 : 25.87
VRL:	0.41 V,	R_s :	53.30 k Ω , R_s/R_0 : 25.87

Figure 19: Results of VRL, R_0 , R_s/R_0 Displayed on Arduino IDE's Serial Monitor

The procedure was repeated for others concentrations: 20ppm, 30ppm, 40ppm, and 50ppm. Because the value obtain is normally logarithmic (MQ135, datasheet, 2022), it is necessary to linearize the values by expressing them into logs. The results were tabulated and the $\log\left(\frac{R_0}{R_s}\right)$, $\log(\text{ppm})$ was also determined as shown in table 2.

Table 2: Known Concentrations (Ppm), Resistances $\left(\frac{R_s}{R_0}\right)$, Log (ppm) And $\log\left(\frac{R_s}{R_0}\right)$

Known Concentrations(ppm)	Resistances $\left(\frac{R_s}{R_0}\right)$	log(ppm)	$\log\left(\frac{R_0}{R_s}\right)$
10	25.88	1.0000	1.4130
20	24.24	1.3010	1.3845
30	23.57	1.4771	1.3723
40	21.75	1.6021	1.3375
50	18.65	1.6990	1.2710

The graph of $\log\left(\frac{R_s}{R_0}\right)$ versus $\log(\text{ppm})$ was plotted in Figure 18. A linear regression was performed, and the slope and intercept of the model was determined, as shown in figure 20.

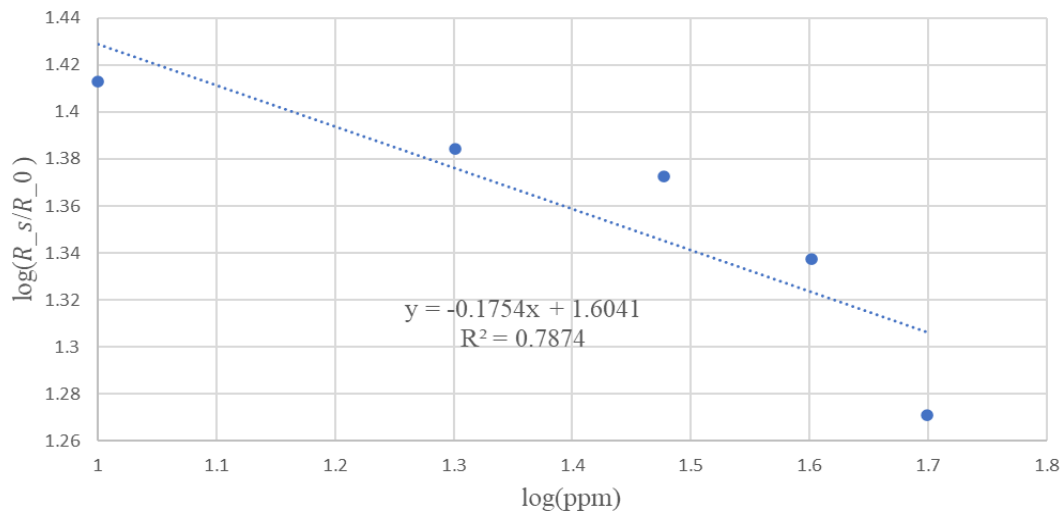


Figure 20: Graph of $\log\left(\frac{R_s}{R_0}\right)$ Versus Log (Ppm)

Based on the regression equation in the graph of $\log\left(\frac{R_s}{R_0}\right)$ versus $\log(\text{ppm})$ (fig.18):

$$y = -0.1755x + 1.6042$$

where:

- $Y = \log\left(\frac{R_s}{R_0}\right)$
- $X = \log(\text{ppm})$

The following observations can be made:

1. Slope = -0.1755

The slope indicates how the value of $\log\left(\frac{R_s}{R_0}\right)$ changes with respect to $\log(\text{ppm})$. A negative slope suggests an inverse relationship between gas concentration and sensor resistance. In this case, as the concentration of NH_3

increases, the sensor resistance R_s decreases (or $\frac{R_s}{R_0}$ decreases). This behavior is typical for metal-oxide sensors like the MQ135, where reduction-oxidation reactions on the sensor's surface lower the resistance as gas concentration increases. A slope of -0.1755 is reasonable for the tested ammonia concentration range (10–50 ppm), though it may vary depending on factors such as temperature, humidity, and the calibrated R_0 value.

2. Intercept = 1.6042

The intercept represents the theoretical value of $\log\left(\frac{R_s}{R_0}\right)$ when $\log(\text{ppm}) = 0$, i.e., when the concentration is 1 ppm. The corresponding $\frac{R_s}{R_0}$ value (antilog of 1.6042) falls within the expected range for the MQ135 sensor in this concentration range. However, this value can also vary depending on the sensor's baseline calibration and environmental conditions, such as temperature and humidity.

3. Coefficient of Determination ($R^2 = 0.7895$)

The R^2 value indicates that approximately 78.95% of the variance in $\log\left(\frac{R_s}{R_0}\right)$ is explained by changes in $\log(\text{ppm})$. This suggests a reasonably good fit of the linear model to the experimental data, though there may still be some variability due to uncontrolled environmental factors or sensor non-linearity at certain ranges. To evaluate the actual level of concentration in ppm using equation 6 and display the temperature and humidity reading, a code was developed. The flowchart of the implemented algorithm is also presented in Figure 21,

$$\text{ppm} = 10^{\frac{R_s/R_0 - \text{Intercept}}{\text{Slope}}}$$

6

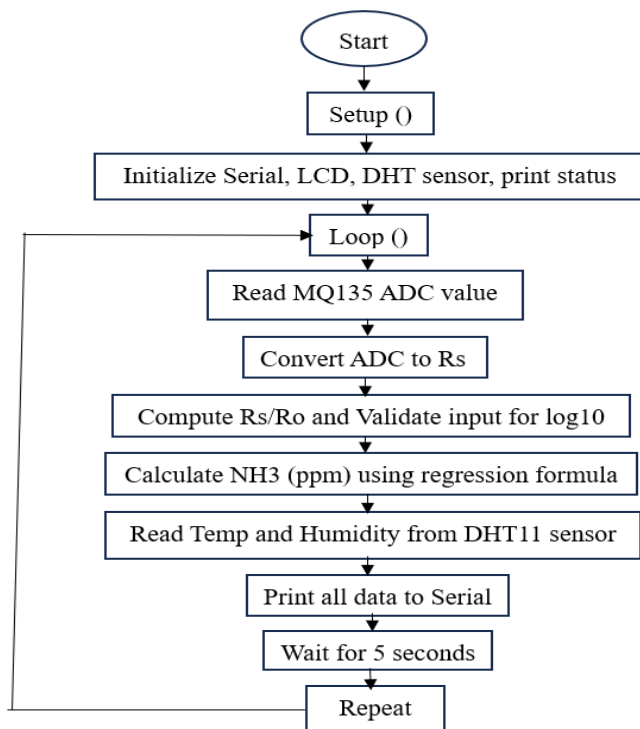
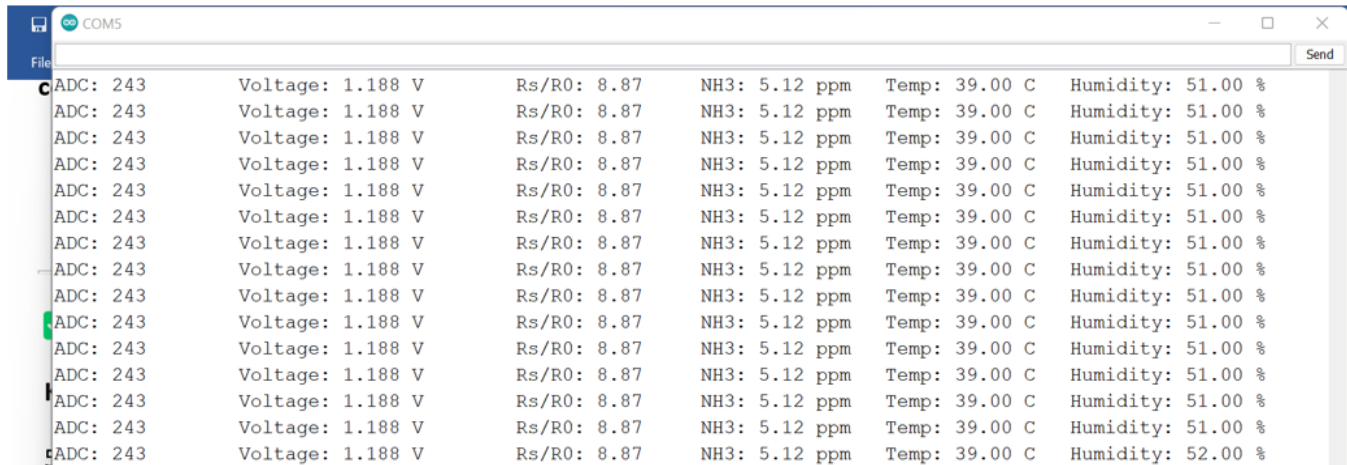


Figure 21: Flowchart of Concentration in ppm, Temperature and Humidity read

Performance assessment of the gas measuring device

After the device was constructed, its performance was evaluated by using it to measure different concentrations of Ammonia. Different quantities of ammonia were tested by the device and the results tabulated in. The result for one of the concentrations (5ppm) is captured in Figure 19. The result also includes the temperature and humidity. The measured concentration was displayed on the Arduino IDE's Serial Monitor, as shown in Figure 21.



ADC	Voltage	Rs/R0	NH3	Temp	Humidity
243	1.188 V	8.87	5.12 ppm	39.00 C	51.00 %
243	1.188 V	8.87	5.12 ppm	39.00 C	51.00 %
243	1.188 V	8.87	5.12 ppm	39.00 C	51.00 %
243	1.188 V	8.87	5.12 ppm	39.00 C	51.00 %
243	1.188 V	8.87	5.12 ppm	39.00 C	51.00 %
243	1.188 V	8.87	5.12 ppm	39.00 C	51.00 %
243	1.188 V	8.87	5.12 ppm	39.00 C	51.00 %
243	1.188 V	8.87	5.12 ppm	39.00 C	51.00 %
243	1.188 V	8.87	5.12 ppm	39.00 C	51.00 %
243	1.188 V	8.87	5.12 ppm	39.00 C	51.00 %
243	1.188 V	8.87	5.12 ppm	39.00 C	51.00 %
243	1.188 V	8.87	5.12 ppm	39.00 C	51.00 %
243	1.188 V	8.87	5.12 ppm	39.00 C	51.00 %
243	1.188 V	8.87	5.12 ppm	39.00 C	51.00 %
243	1.188 V	8.87	5.12 ppm	39.00 C	52.00 %

Figure 21: Sensor’s Measured of 5ppm Known Concentration Result

The procedure was repeated for others known concentrations: 10ppm, 15ppm, 20ppm, 25ppm, 30ppm, 35ppm, 40ppm, 45ppm and 50ppm respectively then sensor's measured data for each concentration was compared with actual known concentrations of NH₃ and calculated the percentage error for each point using equation ,7, as tabulated in table 2.

$$Error(\%) = \left[\frac{Measured\ Concentration - Actual\ Concentration}{Actual\ Concentration} \right] \times 100 \quad 7$$

Table 2: Calculated Percentage Error

Known Concentration(ppm)	Measured Concentration (ppm)	Error (%)
5	5.12	2.40
10	10.45	4.50
15	15.54	3.60
20	20.10	0.50
25	26.05	4.20
30	30.56	1.87
35	35.41	1.17
40	40.17	0.43
45	45.40	0.89
50	48.77	2.46

Evaluation of the systems error

- Minimum Error: 0.43% (at 40 ppm)
- Maximum Error: 4.50% (at 10 ppm)
- Average Error:

$$Average\ Error = \frac{2.40 + 4.50 + 3.60 + 0.50 + 4.20 + 1.87 + 1.17 + 0.43 + 0.89 + 2.46}{10} = 2.11\%$$

DISCUSSION OF RESULTS

The MQ135-based ammonia gas sensor developed in this study performed reliably across a range of tested concentrations, achieving an overall average error of just 2.11%. This level of accuracy makes it a promising low-cost solution for general air quality monitoring, especially for detecting ammonia in indoor or controlled environments.

The sensor demonstrated its highest accuracy within the mid-range concentrations—specifically at 20 ppm (0.50% error), 40 ppm (0.43%), and 45 ppm (0.89%). These results suggest that the calibration curve is most linear and stable in this range, which is particularly relevant for environmental and agricultural monitoring where ammonia levels often fall between 20–45 ppm.

Slightly higher errors were observed at the lower and upper ends of the tested range: 4.50% at 10 ppm and 4.20% at 25 ppm. These discrepancies are consistent with known limitations of MQ-series sensors. As noted by Li *et al.*, (2022), maintaining an error margin below 5% is generally acceptable for practical, non-industrial applications. The increase in error at low concentrations is likely due to the sensor's non-linear behavior in that region, where small changes in gas levels lead to minimal signal variation. Other contributing factors may include analog-to-digital converter (ADC) noise and minor voltage fluctuations, which can affect resolution.

Despite these variations, the sensor's overall performance remained stable, with no abnormal signal spikes or outliers during repeated measurements. This indicates good repeatability and robust mechanical and electrical stability important characteristics for any system designed for ongoing or long-term monitoring.

The findings of this study are consistent with previous research. For example, Moshayedi *et al.*, (2023) reported an average ammonia detection error of 2.5% for the MQ135 within the 10–50 ppm range, with peak accuracy near 30–40 ppm. Similarly, Ogaji *et al.*, (2024) observed increased signal noise at concentrations below 15 ppm, supporting the trends observed in this work. These comparisons further validate the reliability of the current system and its calibration approach, particularly when used within the sensor's optimal operating range.

CONCLUSION

In conclusion, the MQ135-based ammonia gas sensor showed strong overall performance, with its highest accuracy observed in the 20–45 ppm range. Although slight deviations were noted at the lower and upper ends of the concentration spectrum, the measurement errors stayed within acceptable limits for typical air quality monitoring applications. To improve the sensor's reliability—particularly under changing environmental conditions a DHT11 sensor was integrated into the system to monitor temperature and humidity. The data from the DHT11 helps adjust the gas sensor readings, compensating for environmental influences that could otherwise affect accuracy. This integration not only enhances measurement precision but also sets the stage for developing more advanced correction algorithms in future upgrades. While the system performs well, periodic recalibration is still recommended to ensure continued accuracy over time.

REFERENCES

1. Abbas, A. F., & Abdullah, M. Z. (2021). Design and implementation of a smart home gas detection based on mobile network system. *Journal of Engineering and Sustainable Development*, 25(2), 9-16.
2. Ahmarez, D., Widiyanto, A., & Nugroho, S. (2024). Automatic Odor Control System in Broiler Chicken Coops Using MQ-135 And DHT 11 Sensors. Paper presented at the E3S Web of Conferences.
3. Akinwumi, S., Okey-Amadi, O., Ayara, W., & Akinwumi, O. (2024). Eco-friendly Weather Monitoring Device using Arduino Mega and Sensor Integration. Paper presented at the IOP Conference Series: Earth and Environmental Science.
4. Altawell, N. (2021). *Introduction to Machine Olfaction Devices*: Elsevier.
5. Amin, M., Yousuf, M., Attaullah, M., Ahmad, N., Azra, M. N., Lateef, M., Aboelenin, S. M. (2023). Cholinesterase activity as a potential biomarker for neurotoxicity induced by pesticides in vivo exposed *Oreochromis niloticus* (Nile tilapia): assessment tool for organophosphates and synthetic pyrethroids. *Environmental Technology*, 44(14), 2148-2156.
6. Azemi, S. N., Loon, K. W., Amir, A., & Kamalrudin, M. (2021). An IoT-based alarm air quality monitoring system. Paper presented at the *Journal of Physics: Conference Series*.
7. Banerjee, A., Sikdar, B., & Roy, S. (2022). IoT Based Air Pollution Monitoring System. A Project report submitted in partial fulfilment of the requirements for the degree of B. Tech in Electrical Engineering. https://www.rccit.org/students_projects/projects/ee/2022/GR3.pdf.
8. Barrett, S. F. (2020). Arduino Platforms. In *Arduino I: Getting Started* (pp. 33-73): Springer.

9. Behera, S. N., Sharma, M., Aneja, V. P., & Balasubramanian, R. (2013). Ammonia in the atmosphere: a review on emission sources, atmospheric chemistry and deposition on terrestrial bodies. *Environmental Science and Pollution Research*, 20, 8092-8131.
10. Carrillo-Amado, Y. R., Califa-Urquiza, M. A., & Ramón-Valencia, J. A. (2020). Calibration and standardization of air quality measurements using MQ sensors. *Respuestas*, 25(1), 70-77.
11. Carrillo-Amado, Y. R., Califa-Urquiza, M. A., & Ramón-Valencia, J. A. (2020). Calibration and standardization of air quality measurements using MQ sensors. *Respuestas*, 25(1), 70-77.
12. Chodorek, A., Chodorek, R. R., & Yastrebov, A. (2022). The prototype monitoring system for pollution sensing and online visualization with the use of a UAV and a WebRTC-based platform. *Sensors*, 22(4), 1578.
13. Choque, E. A. C., Tapia, J. A. F., Casas, L. A. A., & Choquehuayta, W. N. (2022). IoT platform for level detection of CO₂ in closed environments. Paper presented at the 2022 IEEE ANDESCON.
14. Eranna, G. (2011). *Metal oxide nanostructures as gas sensing devices*: CRC press.
15. Koel, M., & Kaljurand, M. (2019). *Green analytical chemistry 2nd Edition*: Royal society of Chemistry.
16. Kuria, K. P., Robinson, O. O., & Gabriel, M. M. (2020). Monitoring temperature and humidity using Arduino Nano and Module-DHT11 sensor with real time DS3231 data logger and LCD display.
17. Li, J. (2015). *Odor Detection and Quality Evaluation by Machine Olfaction*: North Carolina State University.
18. Li, T., Yin, W., Gao, S., Sun, Y., Xu, P., Wu, S., Wei, G. (2022). The combination of two-dimensional nanomaterials with metal oxide nanoparticles for gas sensors: a review. *Nanomaterials*, 12(6), 982.
19. Mane, S. A., Nadargi, D. Y., Nadargi, J. D., Aldossary, O. M., S. Tamboli, M., & Dhulap, V. P. (2020). Design, development and validation of a portable gas sensor module: A facile approach for monitoring greenhouse gases. *Coatings*, 10(12), 1148.
20. Maulini, R., Sahlinal, D., & Arifin, O. (2022). Monitoring of pH, ammonia (NH₃) and temperature parameters aquaponic water in the 4.0 revolution era. Paper presented at the IOP Conference Series: Earth and Environmental Science.
21. Mohiddin, M., & Kumar, A. (2018). A low-cost air quality monitoring sensor system with Arduino uno micro controller board on smart phone and laptop. *Advances in Industrial Engineering and Management*, 7(2), 22-29.
22. Murawska, A., & Prus, P. (2021). The progress of sustainable management of ammonia emissions from agriculture in European Union States including Poland—Variation, trends, and economic conditions. *Sustainability*, 13(3), 1035.
23. Ogaji, A., Umezurike, O., Imarhiagbe, N., Oriyomi, A., Igbiosa, G., Obiora, G., Ajibola, O. (2024). Design and Implementation of Air Pollution Monitoring WSN System. Paper presented at the 2024 IEEE 5th International Conference on Electro-Computing Technologies for Humanity (NIGERCON).
24. Pecly, J. O. G. (2023). Strategies to obtain a better quality of environmental data gathered by low cost systems. *Environmental Monitoring and Assessment*, 195(2), 289.
25. Petric, M., Dodigović, F., Grčić, I., Markužić, P., Radetić, L., & Topić, M. (2019). Ammonia concentration monitoring using arduino platform. *Environmental Engineering-Inženjerstvo okoliša*, 6(1), 21-26.
26. Rico, J. E., & Turkoglu, K. (2016). Arduino based low-cost experimental unmanned aerial flight system for attitude determination in autonomous flights. Paper presented at the AIAA Modeling and Simulation Technologies Conference.
27. Salam, M. A., & Rahman, Q. M. (2018). *Fundamentals of electrical circuit analysis*: Springer.
28. Seesaard, T., Kamjornkittikoon, K., & Wongchoosuk, C. (2024). A comprehensive review on advancements in sensors for air pollution applications. *Science of The Total Environment*, 175696.
29. Siswanto, S., Anif, M., Hayati, D. N., & Yuhefizar, Y. (2019). Pengamanan pintu ruangan menggunakan arduino mega 2560, mq-2, dht-11 berbasis android. *Jurnal RESTI (Rekayasa Sistem dan Teknologi Informasi)*, 3(1), 66-72
30. Syahputra, R. J., Sihombing, M., & Saripurna, D. (2023). Monitoring The Temperature and Humidity Air In The Room Using A Sensor IoT-Based DHT-11. *Journal of Artificial Intelligence and Engineering Application*, 3(1), 364.

31. Ti, C., Xia, L., Chang, S. X., & Yan, X. (2019). Potential for mitigating global agricultural ammonia emission: a meta-analysis. *Environmental Pollution*, 245, 141-148.
32. Wijaya, D. R., Sarno, R., & Zulaika, E. (2016). Sensor array optimization for mobile electronic nose: Wavelet transform and filter-based feature selection approach. *International Review on Computers and Software*, 11(8), 659-671.
33. Wyer, K. E., Kelleghan, D. B., Blanes-Vidal, V., Schauburger, G., & Curran, T. P. (2022). Ammonia emissions from agriculture and their contribution to fine particulate matter: A review of implications for human health. *Journal of Environmental Management*, 323, 116285.